Treatment planning of electroporation-based medical interventions: electrochemotherapy, gene electrotransfer and irreversible electroporation

Anze Zupanic[1]**, Bor Kos**[1] **and Damijan Miklavcic**

University of Ljubljana, Faculty of Electrical Engineering, Trzaska 25, 1000, Ljubljana, Slovenia

E-mail: damijan.miklavcic@fe.uni-lj.si

Abstract

In recent years, cancer electrochemotherapy (ECT), gene electrotransfer for gene therapy and DNA vaccination (GET) and tissue ablation with irreversible electroporation (IRE) have all entered clinical practice. We present a method for a personalized treatment planning procedure for ECT, GET and IRE, based on medical image analysis, numerical modelling of electroporation and optimization with the genetic algorithm, and several visualization tools for treatment plan assessment. Each treatment plan provides the attending physician with optimal positions of electrodes in the body and electric pulse parameters for optimal electroporation of the target tissues. For the studied case of a deep-seated tumour, the optimal treatment plans for ECT and IRE require at least two electrodes to be inserted into the target tissue, thus lowering the necessary voltage for electroporation and limiting damage to the surrounding healthy tissue. In GET, it is necessary to place the electrodes outside the target tissue to prevent damage to target cells intended to express the transfected genes. The presented treatment planning procedure is a valuable tool for clinical and experimental use and evaluation of electroporation-based treatments.

[S] Online supplementary data available from stacks.iop.org/PMB/57/5425/mmedia

(Some figures may appear in colour only in the online journal)

1. Introduction

When cells are exposed to high electric fields of sufficient magnitude, the cell membrane becomes permeabilized. Electroporation, as the phenomenon has been named, results in inflow/outflow of various molecules that are otherwise unable to cross the membrane (Sale and Hamilton 1967). Usually, the electric fields are induced by electric pulses delivered to

---

[1] Both authors contributed equally to this work.

cells/tissues via needle or plate electrodes; by controlling the electric pulse parameters it is possible to control the level of electroporation, either reversible—caused by electric fields above the reversible but below the irreversible threshold—or irreversible that in time causes cell death (Neumann *et al* 1982). As electroporation is effective regardless of cell type—i.e. it works in prokaryotic and eukaryotic cells, mature neurons, as well as stem cells (Dunny *et al* 1991, Costa *et al* 2007, Jordan *et al* 2008)—it has become a ubiquitous biotechnological and biomedical tool for inducing molecular transport into and out of biological cells (Pakhomov *et al* 2010), with uses ranging from food processing (Morales-de la Peña *et al* 2011, Sack *et al* 2010) and *in utero* gene transfection (Garcia-Frigola *et al* 2007) to medical treatments, such as: (1) cancer electrochemotherapy (ECT) (Marty *et al* 2006, Mir *et al* 1991, Testori *et al* 2011), (2) gene electrotransfer for gene vaccination or gene therapy (GET) (Heller *et al* 2006, Luxembourg *et al* 2007) and (3) tissue ablation with irreversible electroporation (IRE) (Davalos *et al* 2005, Rubinsky *et al* 2007).

Although ECT, IRE and GET all utilize membrane electroporation, the nature of the desired effects requires that different electric pulse parameters be used for each of them. For ECT, it is necessary to reversibly electroporate tumour cells so that chemotherapeutic drugs can enter and cause cell death (Sersa *et al* 2008b). Although sufficient concentration of drugs in the cancer cells is the main cause of cell death, the contribution of irreversible electroporation can sometimes be substantial and is therefore tolerated. In GET, reversible electroporation is necessary to achieve DNA transfer and the resulting expression of therapeutic molecules. However, in contrast to ECT, irreversible electroporation has to be avoided as dead cells do not express the transferred genes; electric fields that generally produce the best results are far below the irreversible electroporation threshold (Gehl *et al* 1999). IRE requires the target tissue to be covered with an electric field above the irreversible electroporation threshold (Rubinsky *et al* 2007); however, the electric field has to be below magnitudes that would cause significant thermal damage (Shafiee *et al* 2009, Zupanic and Miklavcic 2011).

While electroporation of any cell type is possible, the exact parameters necessary for electroporation (i.e. the duration and magnitude of electric field that causes electroporation) of different cell types differ considerably, partly due to their different size and partly due to other cellular, or when electroporating tissues, extracellular biological differences (Kotnik *et al* 1997, Valic *et al* 2003, Kanthou *et al* 2006, Rols and Teissie 1992). Since tissues usually incorporate many different cell types, determining the optimal parameters for each application and for each tissue is both demanding and time consuming (Sel *et al* 2005). Furthermore, knowing the optimal parameters is not enough for successful medical application; it is also necessary to ensure that they are achieved in the whole target tissue and that damage to healthy tissue is kept at a minimum. This requires exact positioning of the electrodes around the target tissue and delivering electric pulses of appropriate amplitude, duration and number. For ECT and IRE, an optimal treatment would include reversible/irreversible electroporation of the whole target volume, while minimizing electroporation of healthy tissues (Miklavcic *et al* 2006). For GET, it is harder to define the exact target volume; however a recent study has demonstrated that it is possible to control the amount of gene expression after transfection by controlling the volume of electroporated tissue (Bureau *et al* 2010); therefore, if the relationship between gene expression and clinical response is known, it can be controlled by the electroporation parameters. It is worth noting that standard operating procedures have been defined for ECT of smaller skin tumours (below 3 cm diameter) that have so far been the main target of ECT, and they include exact guidelines for positioning of the electrodes and the amplitude of electric pulses (Mir *et al* 2006); however, these procedures do not provide guidelines for internal tumours, or tumours of larger dimensions and more complex shapes, which require a more involved pre-treatment planning.

In several recent studies, the utility of numerical modelling in predicting electroporation outcomes has been demonstrated (Miklavcic *et al* 2000, Pavselj *et al* 2005, Sel *et al* 2007, Edd and Davalos 2007, Garcia *et al* 2010, Mahmood and Gehl 2011). Our group is developing a treatment planning procedure for ECT of superficial and deep-seated tumours by combining medical image analysis, finite element modelling of electroporation and a genetic optimization algorithm (Zupanic *et al* 2008, Corovic *et al* 2008, Pavliha *et al* 2012). The genetic algorithm is used to change the location and electric potential of individual electrodes in the numerical models, until a good enough solution is obtained. Recently, we have used the treatment planning procedure for ECT of deep-seated tumours and also analysed the treatment planning robustness to errors in assigned tissue properties and errors in electrode positioning during treatment (Miklavcic *et al* 2010, Kos *et al* 2010). The procedure is currently being tested in a clinical trial of ECT of liver metastases at Institute of Oncology Ljubljana (EudraCT number 2008-008290-54; ClinicalTrials.gov (NCT01264952)) (Edhemovic *et al* 2011).

In this paper, we demonstrate that the treatment planning procedure that has been used before for ECT treatment planning can also be used for GET and IRE treatment planning. We can achieve this, by using the same mathematical model of electroporation and optimization procedures, but with the objective functions defined specifically for each treatment. We also propose several complementary ways of visually presenting the treatment planning data in the clinical environment. Furthermore, by comparing optimization results, we provide general guidance on positioning of the electrodes, including the number of required electrodes inserted in the target tissue.

2. Methods

2.1. How electroporation is performed in current electrochemotherapy clinical trials

The ECT procedure that is the base of the treatment planning algorithm presented in this paper depends on the properties of the equipment used to generate and measure electric pulses—Cliniporator Vitae (IGEA, Carpi, Italy). With Cliniporator Vitae, a train of high-voltage electric pulses is applied on two electrodes (one anode and one cathode) at a time. Currently, eight 100 μs pulses with a repetition frequency of 1 Hz or 5 kHz are used; these are the parameters, for which electroporation thresholds have been determined in several tissues (Miklavcic *et al* 2000). The voltage can be adjusted by the user—medical doctor. If more than two electrodes are inserted into the tissue, trains of pulses can be applied on all possible pairs of electrodes, or only on particular pairs, defined by the treatment plan. In our study, we used 4, 5 or 6 electrodes inserted into the tissue. Electric pulses were applied to most possible pairs; in case of four electrodes, pulses were applied between electrodes 1–2, 1–3, 1–4, 2–3, 2–4 and 3–4. In case of five or six electrodes, more pairs are available and more pulses are thus applied. After all electric pulses are satisfactorily applied during a treatment, the electrodes are removed and the procedure is, for the electroporation part, over.

2.2. Model geometry

The model geometry used in the study was taken from a recent clinical case of ECT of a melanoma metastasis in the thigh of a patient. Briefly (for details, see Miklavcic *et al* (2010)), the model geometry was constructed from 32 CT images of the thigh (slice thickness 2.5 mm and pixel size 1.172 mm), with the tissues in the region of interest (tumour, muscle, fat) first delineated by an expert and then exported into COMSOL Multiphysics (version 3.5a, COMSOL, Sweden) with an algorithm written in Matlab (version 2009a, Mathworks,
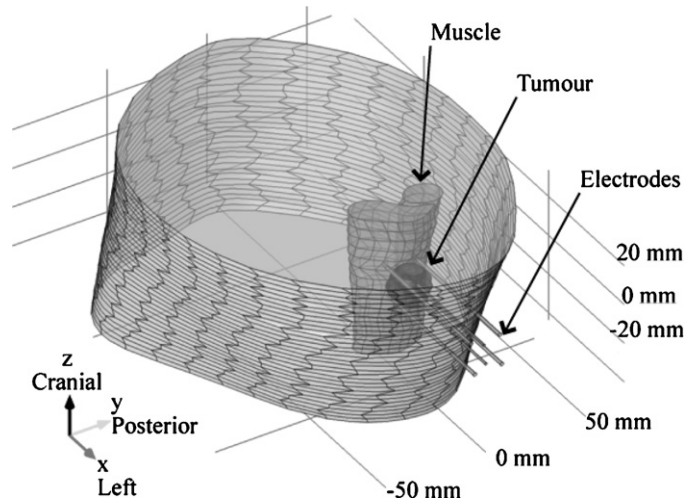
Figure 1. Ortographic representation of the model geometry. The model consists of three tissues and 4–6 electrodes. Given are the scale and the major axes used throughout the paper and the patient-centric directions.

USA). The resulting three-dimensional model, with added electrodes (1.8 mm in diameter and 10 cm in length, with a 4 cm conductive region at the top), is shown in figure 1. All tissues were considered isotropic and homogeneous, with conductivity values, before and during electroporation, and reversible electroporation thresholds the same as in Miklavcic *et al* (2010) and references therein, with the exception of muscle electroporation thresholds that were set lower as a result of recent measurements (Corovic *et al* 2010).

2.3. Mathematical model of electroporation

The sequential model of tissue electroporation that takes into account changes in electrical conductivity in the duration of electric pulses was used for all calculations (Pavselj *et al* 2005, Sel *et al* 2005). Details on the reasoning behind the sequential model and implementation in COMSOL Multiphysics can be found in Pavselj *et al* (2005). Briefly, the sequential model is superior to other current tissue level electroporation models in that it is able to accurately predict the electric current during the pulses and also better predicts the electroporated volume (Sel *et al* 2005). Mathematical simulation of electroporation with the sequential model includes: step 1—solving the Laplace equation for static electric currents:

$$- \nabla \cdot (\sigma \cdot \nabla V) = 0, \tag{2.1}$$

where σ is tissue conductivity and V is electric potential, and the boundary conditions are constant potential ($V = const.$) on the surface of the active parts of the electrodes, continuity ($\boldsymbol{n} \cdot (\boldsymbol{J_1} - \boldsymbol{J_2}) = 0$–*normal current density is continuous on both sides of the boundary*) on all other interior boundaries and insulation ($\boldsymbol{n} \cdot \boldsymbol{J} = 0$–*normal current density across the boundary is zero*) on the inactive parts of the electrodes and outer boundaries of the model, respectively; step 2—irreversibly changing electrical conductivity due to electric fields above the electroporation threshold:

$$\sigma (E) = \frac{\sigma_2 - \sigma_1}{E_{\text{irr}} - E_{\text{rev}}} \cdot E + \sigma_1, \tag{2.2}$$

where σ_1 and σ_2 are electrical conductivities of non-electroporated and electroporated tissues, respectively, and E_{irr} and E_{rev} are the thresholds of irreversible and reversible electroporation, respectively; step 3—sequentially repeating steps 1 and 2 until a steady state, when the conductivity does not change in sequential steps, is reached.

2.4. Optimization

Optimization with a genetic algorithm (Holland 1992) was used to determine the optimum electrode positions and voltages between pairs of electrodes used to deliver the electroporation pulses. The genetic algorithm was written in Matlab and was run together with the finite element models using the link between Matlab and COMSOL Multiphysics. The details of the basic algorithm can be found in Zupanic et al (2008), while here we report the specific implementation and supplemental features. The genetic algorithm works by first defining an initial population of treatment plans (electrode number, positions and voltages applied between all pairs of adjacent electrodes). The quality of the treatment plans is then evaluated using a specifically defined fitness function (see equations (2.4)–(2.6) for the fitness functions used in this study). Treatment plans are, with a probability proportional to their quality, later selected for 'reproduction' by mathematical operations of mutation or cross-over. In this study, the population size was 30, in each generation all solutions except top three (elite) were replaced, and the algorithm ran for 300 iteration before stopping. The mutation rate was 50% (50% cross-over) in the first iteration and then dropped to 5% (95% cross-over) in the last iteration.

When choosing the electrode positions and voltages between the electrode pairs, the following constraints were used: electrodes penetrating the tumour were positioned in parallel, normal to the yz plane (figure 1), 1 cm apart, while electrodes positioned around the tumour had to be more than 0.5 mm and less than 3 cm from the tumour boundary; all electrodes were positioned so that the tip of the electrodes was at the same depth as the deepest part of the tumour; voltages between pairs of electrodes (in clinical ECT electric pulses are delivered sequentially between pairs of electrodes) ranged between 500 and 3000 V, which is the range of Cliniporator Vitae (IGEA, Carpi, Italy), the device currently being used to deliver electric pulses in clinical ECT at the Institute of Oncology in Ljubljana; there was also the option of 0 V between the electrodes, in which case the pair of electrodes was not included in the calculations. By using these constraints we avoided positioning the electrodes at the very edge of the tumour, which has been shown to be extremely difficult in clinical ECT (Miklavcic et al 2010) and also causes problem for the meshing algorithm used in COMSOL Multiphysics. At the same time, we avoided positioning electrodes too far from the tumour, which could not guarantee complete coverage of the tumour with an electric field of sufficiently high magnitude. Additional constraints were the maximum electric current allowed (50 A, Cliniporator Vitae)— when the current exceeded 50 A, the treatment plan's fitness was changed to zero—and the number of used electrodes—limited to 4, 5 or 6. Because it is not possible to cross-over two treatment plans with different numbers of electrodes, the number of electrodes in the 'offspring' was determined randomly. Optimization was also performed using only sets of 4, 5 or 6 electrodes in a single optimization, to determine the efficiency of the algorithm of choosing the correct number of electrodes, but also to compare the optimum solutions in each specific case (it is wise to prepare more than one good enough treatment plan, in case insertion of some electrodes is not possible due to, e.g., the mobility of the tumour (Miklavcic et al 2010)). As the results of the combined optimization (4, 5 or 6 electrodes) did not significantly differ from best treatment plan of individual optimization, we only report the individual results here.

Separate fitness functions were defined for ECT, IRE and GET, after consulting with medical doctors involved in the ECT clinical trial at the Institute of Oncology, Ljubljana. For instance, fitness functions (equation (2.10)) for ECT were set according to the following reasoning:

$$F = \sum_t a_t E_{\text{rev}}^t - \sum_c b_c E_{\text{irr}}^c - \sum_t c_t E_{\text{irr}}^t - \sum_c d_c E_{\text{rev}}^c. \tag{2.3}$$

It is most important to cover all target tissues (^{t}) by an electric field above the reversible thresholds ($_{\text{rev}}$); keeping healthy tissues (^{c}) (in our case, muscle and fat) from being damaged by irreversible electroporation is less important; keeping the tumour from being damaged by the electric field above the irreversible threshold ($_{\text{irr}}$) even less important; and keeping the healthy tissues from being reversibly electroporated is the least important. Therefore the weights in equation (2.3) were set as $a_t > b_c > c_t > d_c$. Similar arguments lead to fitness functions for the optimization of IRE, as seen in the fitness function for ECT (2.4), GET (2.5) and IRE (2.6):

$$F_{\text{ECT}} = 100 \, V_{\text{rev}}^T - 10 \, V_{\text{irr}}^M - 5 \, V_{\text{irr}}^F \tag{2.4}$$

$$F_{\text{GET}} = 100\left(V_{\text{rev}}^T - V_{\text{irr}}^T\right) - 10 \, V_{\text{irr}}^M - 5 \, V_{\text{irr}}^F \tag{2.5}$$

$$F_{\text{IRR}} = 100 \, V_{\text{irr}}^T - 10 \, V_{\text{irr}}^M - 5 \, V_{\text{irr}}^F, \tag{2.6}$$

where (^{T}) is tumour, (^{M}) is muscle and (^{F}) is fat tissue. It should be stressed that the weights chosen for these fitness function are specific for this particular case, namely for a tumour on top muscle tissue, surrounded by fat. If the tumour was located near a vital tissue, such as the heart or the spine, the weights preventing damage to these tissues should be set higher. In general, the weights should be adjusted for each treatment and each patient.

2.5. Visualization

The first visualization approach is the overlay of the original CT images and the output of the model—the increases in tissue conductivity caused by electric field exceeding the electroporation thresholds (figure 2, supplementary file Electroporation_cross_section_images available from stacks.iop.org/PMB/57/5425/mmedia). The overlays were generated in Matlab using the built-in post-processing interpolation function of the COMSOL-Matlab link (postinterp). The function allows for interpolation of any result on an arbitrary three-dimensional grid. This allowed us to extract the results in a grid that corresponds on a pixel-by-pixel level with the original CT images.

The algorithm for extracting the results was as follows. For each subdomain in the COMSOL model (there were a total of two subdomains for the tumour tissue, five subdomains for the muscle tissue and one subdomain for the fat tissue), the interpolation was performed to determine where the conductivity increased. The increase of conductivity in the model is directly related to the maximum electric field strength and consequently also to the degree of electroporation (Pavlin *et al* 2005).

The other visualization approach is the cumulative coverage plot, which represents cumulative coverage of tissues by electric fields above the electroporation threshold after the complete sequence of pulses has been applied (cumulative coverage plot—figure 5). Together with the individual electrode–pair contributions presented in figure 6, these visualizations enable a quantitative means of comparing different treatment plans.
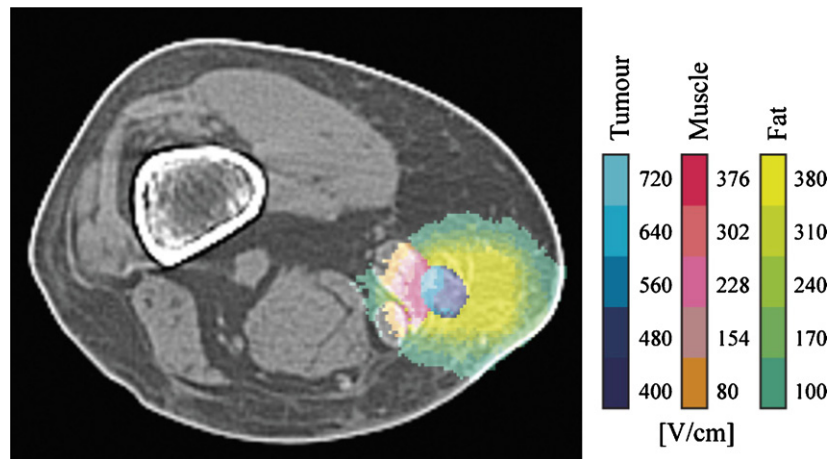
Figure 2. Cross-section plot of electroporation, slice 18 in the original CT images. The cross-section shows the degree of electroporation achieved by the proposed treatment plan for ECT with four electrodes, relative to the maximum reached electric field strength in the cross-section. The overlay consists of three colour progressions, with each colour indicating fields at or above the numerical value indicated in ($V\,cm^{-1}$). The plot also gives an overview of the segmentation of the tissues and a qualitative means of evaluating the solution. Each pixel on the colour overlay represents a volume with dimensions of $1.2 \times 1.2 \times 2.5$ mm.

3. Results

3.1. Treatment plans for ECT, GET and IRE

In this study, we produced nine separate treatment plans, three each for ECT, GET and IRE. For each of the treatments, one treatment plan was prepared for four, one for five, and one for six electrodes inserted into and around the target tissue (in the following text referred to by the initials and number indicating the number of electrodes used, e.g. ECT4 for the four electrode electrochemotherapy). While complete tumour volume electroporation was achieved in all nine treatment plans, there were significant differences in both the optimal positions (figure 3) and voltages between the electrodes (table 1) as well as the total electric current (table 2). The fitness functions and coordinates of electrodes are reported in supplementary data table 1 (available from stacks.iop.org/PMB/57/5425/mmedia).

For ECT, 100 % reversible electroporation of tumour was achieved regardless of the number of electrodes used; however, six electrodes proved to be better than five or four as their use caused the least healthy tissue damage (figure 4). The electric pulses delivered between the intratumoral electrodes already reversibly electroporate most of the tumour volume; therefore, lower voltage can be applied by the electrodes positioned around the tumour, causing less healthy tissue damage. With five electrodes, the penetrating electrode always has a partner electrode outside the tumour volume; because fat tissue surrounding the tumour has lower electrical conductivity than the tumour, a lot of the electric energy is 'lost' via the voltage drop across the fat and therefore higher voltages are needed for electroporation, leading to more healthy tissue damage. For the same reason, the four electrodes treatment plan was the worst of the three.

The IRE treatment plans follow the ECT plans closely, with six electrodes being better than five and four being the worst (in all three electrode configurations complete coverage of the tumour was achieved). The voltages required for IRE are significantly higher than for
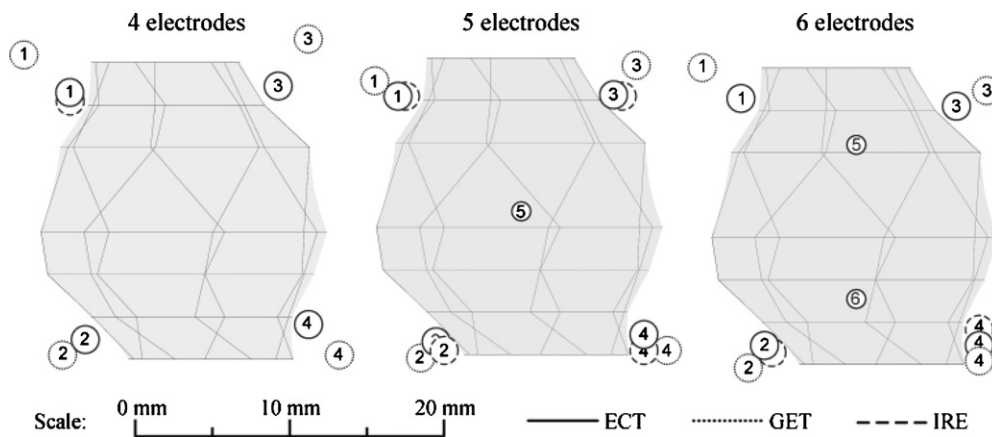
Figure 3. Positions of the electrodes with respect to the tumour for all nine treatment plans. The cross-section shows electrode positions in the *y–z* plane. All elements of the figure are in scale.

Table 1. Voltages between electrode pairs for all nine treatment plans. U_{12} denotes voltage between electrodes 1 and 2; electrode numbering is shown in figure 3.

	4 electrodes			5 electrodes			6 electrodes		
	ECT	GET	IRE	ECT	GET	IRE	ECT	GET	IRE
U_{12} [V]	1100	1500	2400	1100	1500	2300	600	1900	2300
U_{13} [V]	1000	1500	2100	1000	1500	2000	600	1900	2000
U_{24} [V]	1000	1400	2100	900	1500	1900	600	1900	2000
U_{34} [V]	1100	1500	2100	1000	1700	2000	600	1900	1900
U_{14} [V]	1400	1800	2500						
U_{23} [V]	1300	1900	2500						
U_{15} [V]				1000	600	1900	600	600	1600
U_{25} [V]				900	600	1900			
U_{35} [V]				1000	600	1800	500	600	1600
U_{45} [V]				1000	600	1900			
U_{26} [V]							600	600	1500
U_{46} [V]							500	600	1600
U_{56} [V]							1900	500	3000

ECT, with the voltages between the penetrating electrodes reaching 3000 V (table 1), the limit of Cliniporator Vitae. Higher voltages also cause more damage to healthy tissue compared to ECT (figure 4).

In contrast to ECT and IRE, six electrodes were the worst choice for GET, as their use lead to a large volume of the tumour irreversibly electroporated (supplementary file: cumulative coverage plots available from stacks.iop.org/PMB/57/5425/mmedia), resulting in less gene expression, and four electrodes the best choice with the least tumour damage, but not the least healthy tissue damage (figure 5). In all three GET treatment plans, the four extratumoral electrodes were positioned further away from the tumour than for either ECT or IRE (figure 3). While this leads to less irreversible electroporation of the tumour tissue, the damage to healthy tissue was also bigger. For illustration of the differences, we have chosen to present the ECT 4, ECT 6, GET 4 and IRE 6 in figures 6 and 7 as examples of more and less damage to surrounding tissues.
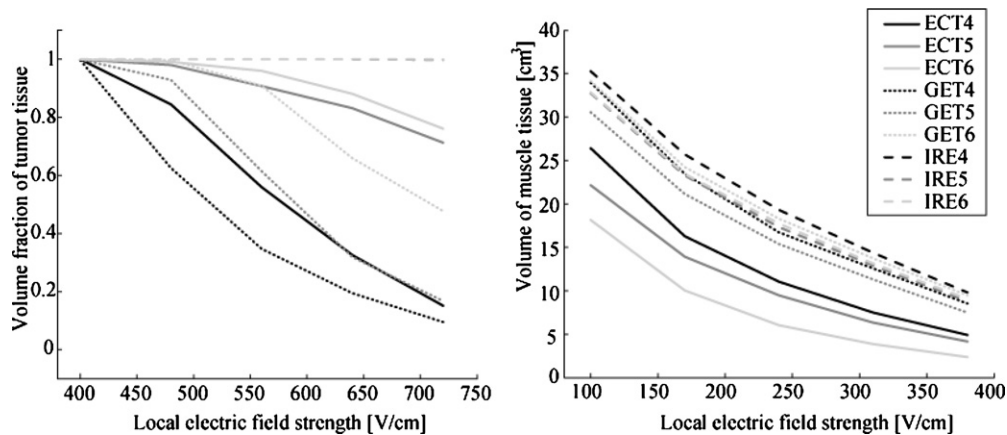
Figure 4. Cumulative coverage plot for the tumour and muscle in all nine treatment plans. Tumour coverage is shown as the fraction of the total volume of the tumour, while muscle is shown as total volume. A similar plot has been produced for the fat tissue, and is available in the supplementary data file—cumulative coverage plots available from stacks.iop.org/PMB/57/5425/mmedia.

Table 2. Computed currents in all nine treatment plans. I_{12} denotes current between electrodes 1 and 2. Electrode numbering is illustrated in figure 3, while the corresponding applied voltages are detailed in table 1.

	4 electrodes			5 electrodes			6 electrodes		
	ECT	GET	IRE	ECT	GET	IRE	ECT	GET	IRE
I_{12} [A]	11.7	13.6	28.7	10.9	13.1	25.4	5.25	15.7	26.1
I_{13} [A]	9.86	12.0	23.5	9.48	12.6	21.4	4.91	15.0	22.0
I_{24} [A]	8.60	9.93	20.7	8.11	12.4	19.8	4.71	18.6	21.9
I_{34} [A]	10.3	10.8	21.7	10.0	15.4	21.5	5.45	19.8	22.5
I_{14} [A]	11.6	11.2	23.3						
I_{23} [A]	12.3	16.5	27.1						
I_{15} [A]				11.5	4.62	24.3	7.09	4.71	22.1
I_{25} [A]				11.4	5.71	26.7			
I_{35} [A]				13.3	5.65	25.7	6.41	6.34	24.5
I_{45} [A]				11.1	4.48	22.3			
I_{26} [A]							8.08	6.61	23.6
I_{46} [A]							5.16	6.46	21.4
I_{56} [A]							30.6	5.44	49.5

3.2. Visualization of the treatment plans

To enable a more visual and information rich comparison of the treatment plans, the modelling results can be overlaid over the original CT images (figure 5) and the coverage of the target and critical tissues by electroporation can be presented in the form of cumulative coverage plots (figures 6 and 7). The curves (figure 6) show the fraction of the tumour volume covered by at least a certain magnitude of electric field (similar to the dose–volume histogram used in radiotherapy (Bevilacqua *et al* 2007). They can be used to relatively quickly evaluate the robustness of the treatment plan, but lack any spatial anatomical detail. Cumulative coverage curves for all nine treatment plans are available in the supplementary file—cumulative coverage plots available from stacks.iop.org/PMB/57/5425/mmedia.
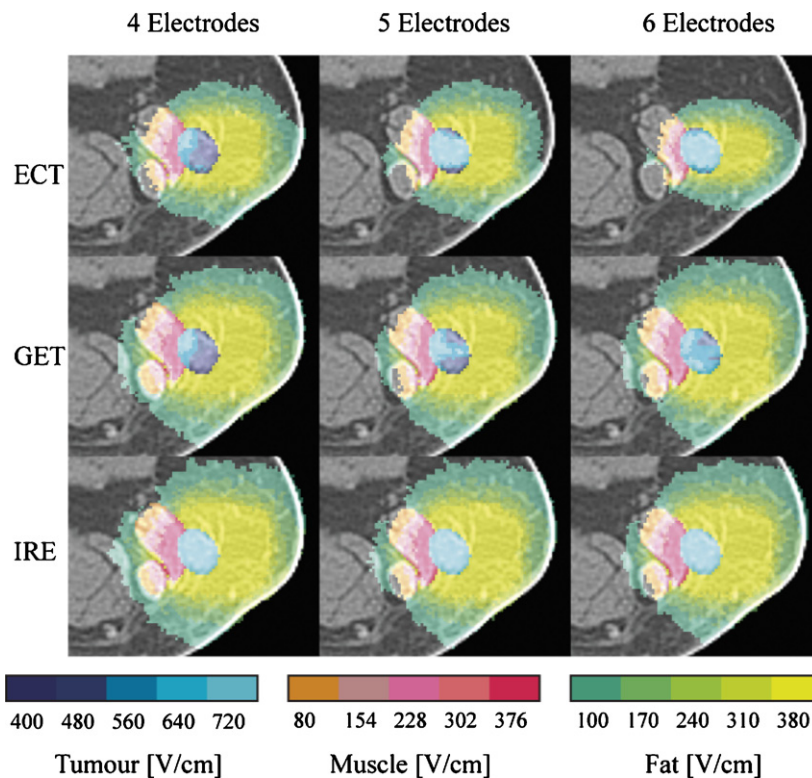
Figure 5. Comparison of the different treatment modalities and electrode configurations. The figure shows the region-of-interest on slice 18. The colour progressions indicate tissue where the electric fields exceed the indicated field strength corresponding to degrees of electroporation.

Additionally, the electrode pair contribution graphs indicate the extent of contribution of each electrode pair towards the total coverage of the target tissue. The CT and modelling overlay provides the spatial details and enables the attending physician to determine regions of the target and healthy tissue, where coverage needs to be improved. For example, in figure 5 it is easy to see that the edges of the tumour in ECT5 are covered by a lower electric field than in ECT6, and, in GET4, that the tumour volume closer to the muscle tissue is irreversibly electroporated, while the volume closer to the skin is reversibly electroporated.

4. Discussion

In recent years electroporation-based treatments have made big steps from the lab into the clinic, with ECT already used for cancer treatment, with three thousand patients treated since SOP were published with success rates over 70% (Marty *et al* 2006, Sersa *et al* 2009, Campana *et al* 2008). As both IRE and GET are also coming closer to clinical use, it is important that the physical part of the treatments—the delivery of electric pulses—is as accurate as possible to give the best chance for complete therapy success. In this study, we demonstrate that the treatment planning procedure originally developed for clinical ECT (Zupanic *et al* 2008, Miklavcic *et al* 2010, Edhemovic *et al* 2011) is also suitable for treatment planning of IRE
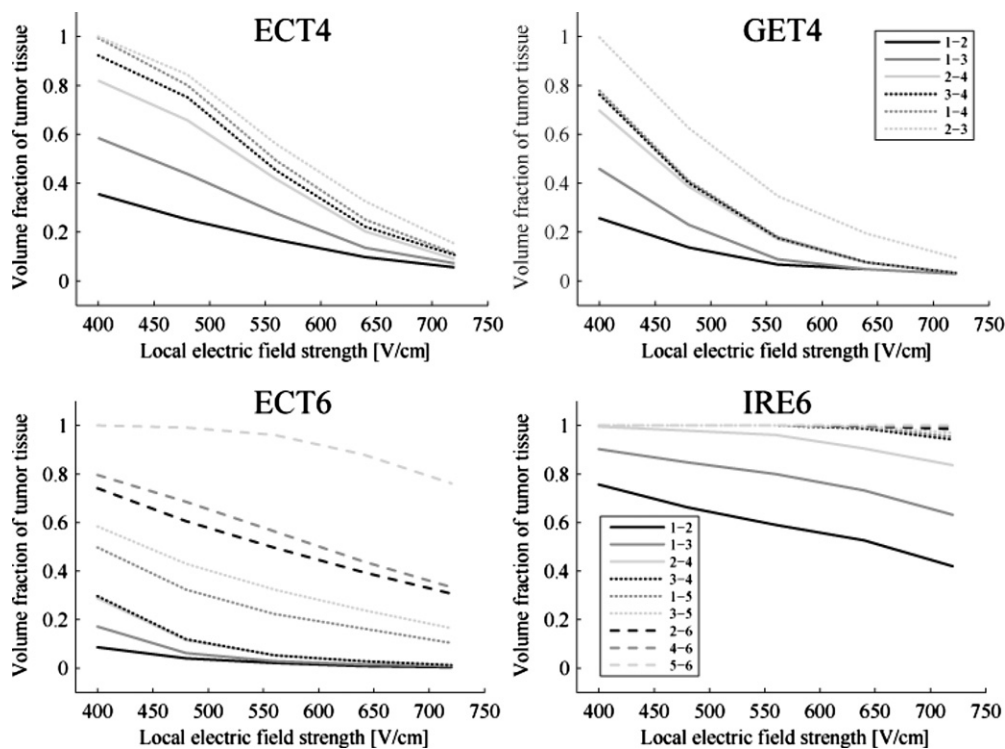
Figure 6. Cumulative coverage plots show the progression of total coverage of the tumour after the train of electric pulses is applied through each new electrode pair. The order in which the contributions were evaluated is the same as in the optimization. The numeral next to the name of the treatment indicates the number of electrodes used.

and GET, albeit with certain modifications in the form of the fitness function used in the optimization process.

By changing the factors and weights of the fitness function (see equations (2.2)–(2.6) in section 2) the treatment plans obtained for ECT, IRE and GET differ considerably. For both ECT and IRE, the best possible electrode configuration used six electrodes, two of them penetrating through the centre of the tumour. By having the entire source (the cathode and the anode) of the electric field inside the tumour the delivered electric energy stays in the tumour; thereby electroporation is limited almost entirely to the tumour volume. Although our study is limited by a single geometry, it is most probable that having two (or more) electrodes inserted into the tumour is the optimal electrode configuration for ECT or IRE of most large target tissues. The electrodes positioned outside the tumour (but still very close, see figure 3) can therefore be used with lower voltages (table 1) with their main function being electroporation of the tumour margins. When only one intratumoral electrode is used, the voltages used on the electrodes outside the tumour have to be higher thereby causing more tissue damage (table 1). Similar conclusions have been reached in a recent study of intracranial IRE, where positioning electrodes inside the target tissue produced better results (Garcia *et al* 2010).

The situation was reversed for GET, with four electrodes being the best option. This was mostly due to irreversible electroporation of the tumour being highly penalized in the fitness function (equation 2.5). A secondary effect of the high penalization was that the outside
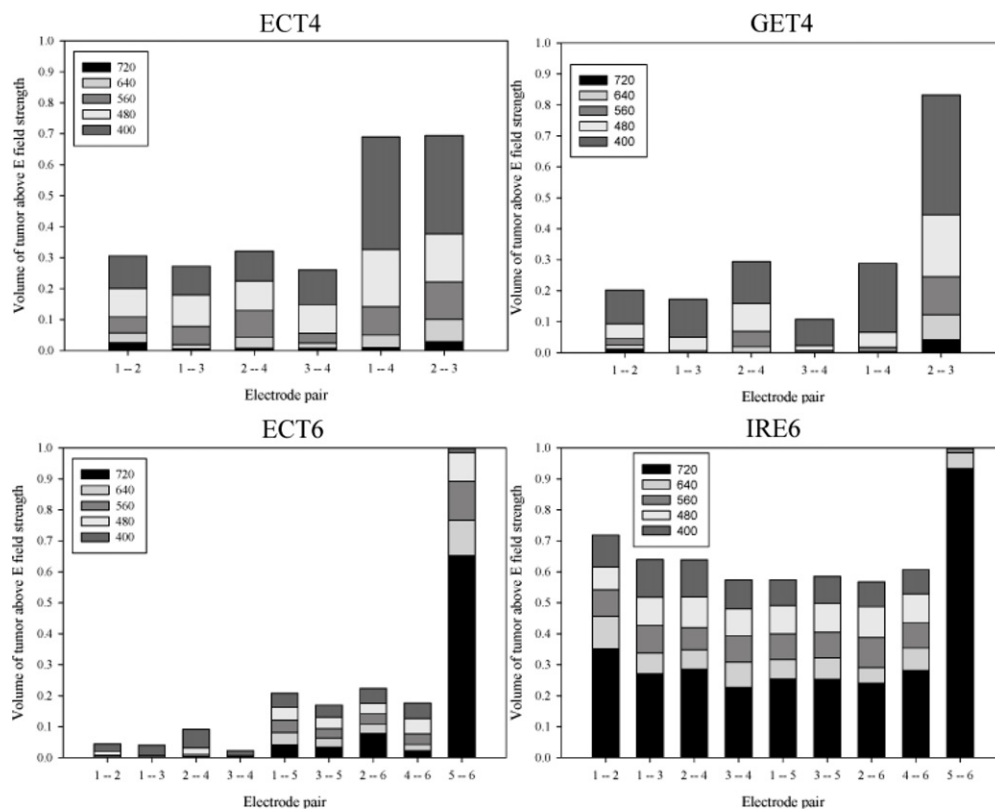
Figure 7. Individual electrode–pair contributions. This figure enables the viewer to discern the contribution of each electrode pair toward the success of the treatment. The values are given in V cm^{-1}. The bars represent the volume fraction of tumour tissue above the respective electric field strength. The numeral next to the name of the treatment indicates the number of electrodes used.

electrodes were positioned further from the tumour than in ECT and IRE; such positioning caused more healthy tissue damage, but less damage to the tumour that was the designated tissue of transfected gene expression. Although the whole tumour volume is not the only possible target for cancer gene therapy (Heller and Heller 2010), the positioning of the electrodes further from the target tissue should remain valid in all cases, where the location of target cells can be volumetrically defined, e.g. stromal cell in the bone marrow (Van Damme *et al* 2002). In other cases, e.g. when muscle is the target tissue, controlling the volume of reversibly electroporated tissue can also control the amount of gene expression (Bureau *et al* 2010), while at the same minimizing damage to the healthy tissue (Zupanic *et al* 2010, Hojman *et al* 2011).

A second important contribution of this research is the presented visualization approach, which gives a new set of tools for the use in the clinical setting as well as for the electroporation research community. It lends itself to easy automation for high-throughput evaluation of treatment plans, and prepares the setting for the discussion on the fitness functions for a more formalized approach to treatment planning. Furthermore, the visualization tools will allow researchers to revisit the subject of robustness of the treatment plans.

The quality of the treatment plans, however, also depends on the validity of the mathematical model of electroporation used. While the current models take into account the

changes in electrical conductivity due to electroporation, and thus considerably improve the prediction of electroporated volumes (Sel *et al* 2005), all tissues are considered homogeneous, which might not be the case in reality. In particular, the viable and necrotic regions of large tumours might have different electrical conductivities. Nevertheless, we believe that a homogeneous representation of the tissues is a good approximation of reality and at the same time the best option currently available, as to the best of our knowledge an estimate of electrical heterogeneity of tumours, does not exist so far. It is, however, consistently reported in the literature that the electric conductivity of tumours is higher than that of the surrounding tissue and our previous investigation has shown that treatment planning depends more on the ratio between conductivities of the tumour and surrounding tissues than small variation of conductivity in the target tissue (Kos *et al* 2010).

Appropriate choice of weights in the fitness function can also significantly influence the quality of the treatment plan; therefore, the weights should be chosen in consultation with the treating medical doctor. When more data from more clinical studies become available, it will be possible to determine a formal way of selecting weights for different electroporation-based treatments, with a high degree of certainty about the quality of the treatment plan. At the moment, the data are not yet available; therefore, we have to rely (only) on critical thinking and knowledge about human physiology.

Our study shows that it is possible to use treatment planning for all three electroporation-based treatments; however, additional research will have to be done before it can be used in for clinical IRE and GET. Namely, the thresholds used in this study are valid only for the case of eight 100 μs pulses (1 Hz repetition frequency) that are currently used in clinical ECT (Sel *et al* 2005), while the pulses used in IRE and GET are different: more pulses and higher/lower repetition frequencies are used in IRE (Rubinsky *et al* 2007, Onik *et al* 2007), while many different pulse configurations are used in GET (Gehl 2003, Rols and Teissie 1998, Bettan *et al* 2000, Satkauskas *et al* 2005, Tevz *et al* 2009, Scheerlinck *et al* 2004). Instead of using the maximum electric field achieved in the tissue as the measure of electroporation (figure 4), it would be better to calculate the probability of electroporation due to exposure to electric pulses. Some steps in this direction were taken in recent studies of the effects of pulse number and duration on electroporation (Golberg and Rubinsky 2010, Pucihar *et al* 2011). Also, since it has been shown several times that the direction of the field is also important— exposing cells or tissue to an electric field from two perpendicular directions and increasing the level of electroporation compared to a single direction (Faurie *et al* 2010, Rebersek *et al* 2007, Valic *et al* 2003)—it would be useful to add directionality to the calculation of the probability.

5. Conclusions

The method presented here enables accurate planning of the electroporation part of ECT, GET for gene therapy and DNA vaccination and IRE. While fixed-geometry electrodes and standard voltages can provide good guidelines in the treatment of smaller skin tumours (Sersa *et al* 2011), we believe that electric field distribution calculations or full treatment planning should be performed before each experiment or clinical treatment of larger target tissues. With all the confounding factors that are currently beyond clinical control, such as the effects of the vascularization on the drug distribution in the target tissues (Sersa *et al* 2008a, Brown *et al* 2004, Jain 1999) or the intrinsic ability of the cells to express the transfected construct (Herweijer and Wolff 2003), it is vital that the electroporation of the target tissues is achieved with certainty.

Acknowledgments

References

Bettan M, Ivanov M A, Mir L M, Boissiere F, Delaere P and Scherman D 2000 Efficient DNA electrotransfer into tumors *Bioelectrochemistry* **52** 83–90

Bevilacqua V, Mastronardi G and Piscopo G 2007 Evolutionary approach to inverse planning in coplanar radiotherapy *Image Vis. Comput.* **25** 196–203

Brown E B, Boucher Y, Nasser S and Jain R K 2004 Measurement of macromolecular diffusion coefficients in human tumors *Microvasc. Res.* **67** 231–6

Bureau M F, Juge L, Seguin J, Rager M-N, Scherman D and Mignet N 2010 Muscle transfection and permeabilization induced by electrotransfer or pluronic® L64: Paired study by optical imaging and MRI *Biochim. Biophys. Acta* **1800** 537–43

Campana L G, Mocellin S, Basso M, Puccetti O, De Salvo G L, Chiarion-Sileni V, Vecchiato A, Corti L, Rossi C R and Nitti D 2008 Bleomycin-based electrochemotherapy: clinical outcome from a single institution's experience with 52 patients *Ann. Surg. Oncol.* **16** 191–9

Corovic S, Zupanic A, Kranjc S, Al Sakere B, Leroy-Willig A, Mir L M and Miklavcic D 2010 The influence of skeletal muscle anisotropy on electroporation: *in vivo* study and numerical modeling *Med. Biol. Eng. Comput.* **48** 637–48

Corovic S, Zupanic A and Miklavcic D 2008 Numerical modeling and optimization of electric field distribution in subcutaneous tumor treated with electrochemotherapy using needle electrodes *IEEE Trans. Plasma. Sci.* **36** 1665–72

Costa M *et al* 2007 A method for genetic modification of human embryonic stem cells using electroporation *Nat. Protoc.* **2** 792–6

Davalos R V, Mir L M and Rubinsky B 2005 Tissue ablation with irreversible electroporation *Ann. Biomed. Eng.* **33** 223–31

Dunny G M, Lee L N and LeBlanc D J 1991 Improved electroporation and cloning vector system for Gram-positive bacteria *Appl. Environ. Microbiol.* **57** 1194–201

Edd J F and Davalos R V 2007 Mathematical modeling of irreversible electroporation for treatment planning *Technol. Cancer Res. Treat.* **6** 275–86

Edhemovic I *et al* 2011 Electrochemotherapy: a new technological approach in treatment of metastases in the liver *Technol. Cancer Res. Treat.* **10** 475–85

Faurie C, Rebersek M, Golzio M, Kanduser M, Escoffre J-M, Pavlin M, Teissie J, Miklavcic D and Rols M-P 2010 Electro-mediated gene transfer and expression are controlled by the life-time of DNA/membrane complex formation *J. Gene Med.* **12** 117–25

Garcia P A, Rossmeisl J H, Neal R E, Ellis T L, Olson J D, Henao-Guerrero N, Robertson J and Davalos R V 2010 Intracranial nonthermal irreversible electroporation: *in vivo* analysis *J. Membr. Biol.* **236** 127–36

Garcia-Frigola C, Carreres M I, Vegar C and Herrera E 2007 Gene delivery into mouse retinal ganglion cells by in utero electroporation *BMC Develop. Biol.* **7** 103

Gehl J 2003 Electroporation: theory and methods, perspectives for drug delivery, gene therapy and research *Acta Physiol. Scand.* **177** 437–47

Gehl J, Sorensen T H, Nielsen K, Raskmark P, Nielsen S L, Skovsgaard T and Mir L M 1999 *In vivo* electroporation of skeletal muscle: threshold, efficacy and relation to electric field distribution *Biochim. Biophys. Acta* **1428** 233–40

Golberg A and Rubinsky B 2010 A statistical model for multidimensional irreversible electroporation cell death in tissue *Biomed. Eng. Online* **9** 13

Heller L and Heller R 2010 Electroporation gene therapy preclinical and clinical trials for melanoma *Curr. Gene Ther.* **10** 312–7

Heller R, Deconti R, Messina J, Andrews S, Urbas P, Ugen K, Puleo C, Sondak V, Riker A and Daud A 2006 Gene therapy with plasmid IL-12 delivered by electroporation in patients with malignant melanoma: results of first human Phase I trial *Eur. J. Cancer Suppl.* **4** 106–106

Herweijer H and Wolff J A 2003 Progress and prospects: naked DNA gene transfer and therapy *Gene Ther.* **10** 453–8

Hojman P, Brolin C and Gissel H 2011 Calcium influx and the muscular response to electrotransfer *Am. J. Physiol. Regul. Integr. Comp. Physiol.* **302** R446–53

Holland J H 1992 *Adaptation in Natural and Artificial Systems: An Introductory Analysis with Applications to Biology, Control, and Artificial Intelligence* (Cambridge: MIT Press)

Jain R K 1999 Transport of molecules, particles, and cells in solid tumors *Ann. Rev. Biomed. Eng.* **1** 241–63

Jordan E T, Collins M, Terefe J, Ugozzoli L and Rubio T 2008 Optimizing electroporation conditions in primary and other difficult-to-transfect cells *J. Biomol. Tech.* **19** 328–34

Kanthou C, Kranjc S, Sersa G, Tozer G, Zupanic A and Cemazar M 2006 The endothelial cytoskeleton as a target of electroporation-based therapies *Mol. Cancer Ther.* **5** 3145–52

Kos B, Zupanic A, Kotnik T, Snoj M, Sersa G and Miklavcic D 2010 Robustness of treatment planning for electrochemotherapy of deep-seated tumors *J. Memb. Biol.* **236** 147–53

Kotnik T, Bobanovic F and Miklavcic D 1997 Sensitivity of transmembrane voltage induced by applied electric fields—a theoretical analysis *Bioelectrochem. Bioenerg.* **43** 285–91

Luxembourg A, Evans C and Hannaman D 2007 Electroporation-based DNA immunisation: translation to the clinic *Exp. Opin. Biol. Ther.* **7** 1647–64

Mahmood F and Gehl J 2011 Optimizing clinical performance and geometrical robustness of a new electrode device for intracranial tumor electroporation *Bioelectrochemistry* **81** 10–6

Marty M, Sersa G, Garbay J, Gehl J, Collins C, Snoj M, Billard V, Geertsen P, Larkin J and Miklavcic D 2006 Electrochemotherapy—an easy, highly effective and safe treatment of cutaneous and subcutaneous metastases: results of ESOPE (European standard operating procedures of electrochemotherapy) study *Eur. J. Cancer Suppl.* **4** 3–13

Miklavcic D, Corovic S, Pucihar G and Pavselj N 2006 Importance of tumour coverage by sufficiently high local electric field for effective electrochemotherapy *Eur. J. Cancer Suppl.* **4** 45–51

Miklavcic D, Semrov D, Mekid H and Mir L M 2000 A validated model of *in vivo* electric field distribution in tissues for electrochemotherapy and for DNA electrotransfer for gene therapy *Biochim. Biophys. Acta* **1523** 73–83

Miklavcic D, Snoj M, Zupanic A, Kos B, Cemazar M, Kropivnik M, Bracko M, Pecnik T, Gadzijev E and Sersa G 2010 Towards treatment planning and treatment of deep-seated solid tumors by electrochemotherapy *Biomed. Eng.* **9** 10

Mir L M, Gehl J, Sersa G, Collins C G, Garbay J R, Billard V, Geertsen P F, Rudolf Z, O'Sullivan G C and Marty M 2006 Standard operating procedures of the electrochemotherapy: instructions for the use of bleomycin or cisplatin administered either systemically or locally and electric pulses delivered by the Cliniporator (TM) by means of invasive or non-invasive electrodes *Eur. J. Cancer Suppl.* **4** 14–25

Mir L M, Orlowski S, Belehradek J and Paoletti C 1991 Electrochemotherapy potentiation of antitumor effect of bleomycin by local electric pulses *Eur. J. Cancer* **27** 68–72

Morales-de la Peña M, Elez-Martínez P and Martín-Belloso O 2011 Food preservation by pulsed electric fields: an engineering perspective *Food Eng. Rev.* **3** 94–107

Neumann E, Schaeferridder M, Wang Y and Hofschneider P H 1982 Gene-transfer into mouse lyoma cells by electroporation in high electric-fields *EMBO J.* **1** 841–5

Onik G, Mikus P and Rubinsky B 2007 Irreversible electroporation: implications for prostate ablation *Technol. Cancer Res. Treat.* **6** 295–300

Pakhomov A G, Miklavcic D and Markov M S 2010 *Advanced Electroporation Techniques in Biology and Medicine* (Boca Raton, FL: CRC Press)

Pavliha D, Kos B, Županič A, Marčan M, Serša G and Miklavčič D 2012 Patient-specific treatment planning of electrochemotherapy: procedure design and possible pitfalls *Bioelectrochemistry* [Epub ahead of print, doi:10.1016/j.bioelechem.2012.01.007]

Pavlin M, Kanduser M, Rebersek M, Pucihar G, Hart F X, Magjarevic R and Miklavcic D 2005 Effect of cell electroporation on the conductivity of a cell suspension *Biophys. J.* **88** 4378–90

Pavselj N, Bregar Z, Cukjati D, Batiuskaite D, Mir L M and Miklavcic D 2005 The course of tissue permeabilization studied on a mathematical model of a subcutaneous tumor in small animals *IEEE Trans. Biomed. Eng.* **52** 1373–81

Pucihar G, Krmelj J, Rebersek M, Napotnik T and Miklavcic D 2011 Equivalent pulse parameters for electroporation *IEEE Trans. Biomed. Eng.* **58** 3279–88

Rebersek M, Faurie C, Kanduser M, Xorovic S, Teissie J, Rols M P and Miklavcic D 2007 Electroporator with automatic change of electric field direction improves gene electrotransfer *in-vitro Biomed. Eng. Online* **6** 25

Rols M P and Teissie J 1992 Experimental-evidence for the involvement of the cytoskeleton in mammalian-cell electropermeabilization *Biochim. Biophys. Acta* **1111** 45–50

Rols M P and Teissie J 1998 Electropermeabilization of mammalian cells to macromolecules: control by pulse duration *Biophys. J.* **75** 1415–23

Rubinsky B, Onik G and Mikus P 2007 Irreversible electroporation: a new ablation modality—clinical implications *Technol. Cancer Res. Treat.* **6** 37–48

Sack M, Sigler J, Frenzel S, Eing C, Arnold J, Michelberger T, Frey W, Attmann F, Stukenbrock L and Müller G 2010 Research on industrial-scale electroporation devices fostering the extraction of substances from biological tissue *Food Eng. Rev.* **2** 147–56

Sale A and Hamilton W 1967 Effects of electric fields on microorganizms I killing of bacteria and yeasts *Biochim. Biophys. Acta* **148** 781–8

Satkauskas S, Andre F, Bureau M F, Scherman D, Miklavcic D and Mir L M 2005 Electrophoretic component of electric pulses determines the efficacy of *in vivo* DNA electrotransfer *Human Gene Ther.* **16** 1194–201

Scheerlinck J P Y, Karlis J, Tjelle T E, Presidente P J A, Mathiesen I and Newton S E 2004 *In vivo* electroporation improves immune responses to DNA vaccination in sheep *Vaccine* **22** 1820–5

Sel D, Cukjati D, Batiuskaite D, Slivnik T, Mir L M and Miklavcic D 2005 Sequential finite element model of tissue electropermeabilization *IEEE Trans. Biomed. Eng.* **52** 816–27

Sel D, Lebar A M and Miklavcic D 2007 Feasibility of employing model-based optimization of pulse amplitude and electrode distance for effective tumor electropermeabilization *IEEE Trans. Biomed. Eng.* **54** 773–81

Sersa G, Cemazar M and Snoj M 2009 Electrochemotherapy of tumours *Curr. Oncol.* **16** 34–5

Sersa G, Gehl J, Garbay J-R, Soden D M, O'Sullivan G C, Matthiessen L W, Snoj M and Mir L M 2011 *Electrochemotherapy of small tumors; the experience from the ESOPE (European standard operating procedures for electrochemotherapy) group* Clinical Aspects of Electroporation ed S T Kee, J Gehl and E W Lee (New York: Springer) pp 93–102

Sersa G *et al* 2008a Vascular disrupting action of electroporation and electrochemotherapy with bleomycin in murine sarcoma *Br. J. Cancer* **98** 388–98

Sersa G, Miklavcic D, Cemazar M, Rudolf Z, Pucihar G and Snoj M 2008b Electrochemotherapy in treatment of tumours *Eur. J. Surg. Oncol.* **34** 232–40

Shafiee H, Garcia P A and Davalos R V 2009 A preliminary study to delineate irreversible electroporation from thermal damage using the arrhenius equation *Trans. ASME, J. Biomech. Eng.* **131** 5

Testori A, Faries M B, Thompson J F, Pennacchioli E, Deroose J P, van Geel A N, Verhoef C, Verrecchia F and Soteldo J 2011 Local and intralesional therapy of in-transit melanoma metastases *J. Surg. Oncol.* **104** 391–6

Tevz G, Kranjc S, Cemazar M, Kamensek U, Coer A, Krzan M, Vidic S, Pavlin D and Sersa G 2009 Controlled systemic release of interleukin-12 after gene electrotransfer to muscle for cancer gene therapy alone or in combination with ionizing radiation in murine sarcomas *J. Gene Med.* **11** 1125–37

Valic B, Golzio M, Pavlin M, Schatz A, Faurie C, Gabriel B, Teissie J, Rols M P and Miklavcic D 2003 Effect of electric field induced transmembrane potential on spheroidal cells: theory and experiment *Eur. Biophys. J.* **32** 519–28

Van Damme A, Vanden Driessche T, Collen D and Chuah M K L 2002 Bone marrow stromal cells as targets for gene therapy *Curr. Gene Ther.* **2** 195–209

Zupanic A, Corovic S and Miklavcic D 2008 Optimization of electrode position and electric pulse amplitude in electrochemotherapy *Radiol. Oncol.* **42** 93–101

Zupanic A, Corovic S, Miklavcic D and Pavlin M 2010 Numerical optimization of gene electrotransfer into muscle tissue *Biomed. Eng. Online* **9** 66

Zupanic A and Miklavcic D 2011 Tissue heating during tumor ablation with irreversible electroporation *J. Electr. Eng. Comput. Sci.* **78** 42–7